Amplification of frequency-swept signals in a W-band gyrotron travelling wave amplifier

Liang Zhang, Craig R. Donaldson, Peter Cain, Adrian W. Cross, and Wenlong He

***Abstract*—The frequency agility of a W-band gyrotron travelling wave amplifier (gyro-TWA) was demonstrated by the amplification of a frequency-swept input signal (chirp signal). The gyro-TWA was developed to provide high output power and wide bandwidth by using a helically corrugated interaction region. In the experiment a ~0.5 W signal of linearly swept frequency bandwidth of 1 GHz was amplified and a gain of over 30 dB was measured when driven by a 40 keV, 1.5 A, axis-encircling electron beam.**

***Index Terms*—gyrotron travelling-wave amplifier, helically corrugated waveguide, gyro-devices, frequency-swept signal.**

I. Introduction

HIGH power amplifiers operating in the millimeter wave (mm-wave) and terahertz frequency ranges are greatly needed in the areas of remote sensing, radar imaging, point-to-point communications, electron spin resonance (ESR) spectroscopy and plasma diagnostics. The "slow wave" devices based on conventional rectilinear electron beams in vacuum electronic devices (VED) such as travelling wave tubes and klystrons are limited by their power capability at high frequency due to the small cross section of the beam-wave interaction as well as the small beam current that can pass through the VED [1]. The gyrotron devices benefit from a "fast wave" interaction based on the cyclotron resonance maser instability. A circular interaction region can therefore be used which allows a much larger power capability [2]. Gyrotron traveling wave amplifiers (gyro-TWAs) [3-5] are a member of the gyro-device family and are able to precisely control amplitude and phase.

Gyro-TWAs based on helically corrugated interaction region (HCIR) have the advantage of wide gain bandwidth. The HCIR has both azimuthal and axial periodicities, which allows resonant coupling between two modes to generate new eigenwaves [6-8]. By choosing appropriate dimensions, different dispersion curves could be obtained for applications such as gyro-BWOs [9, 10], gyro-TWAs [11-13], microwave pulse compressors [14, 15] and mode converters [16, 17]. When a three-fold HCIR was used in a gyro-TWA, the eigenwave was coupled between the TE_{21} mode and the first spatial harmonic of the TE_{11} mode. The dispersion curve could be optimized to achieve a nearly constant group velocity at small wavenumber values and across a large frequency bandwidth. Another advantage of the HCIR is that the beam-wave interaction occurs at the 2nd cyclotron harmonic, therefore the required magnetic field can be halved as compared with operation at the fundamental harmonic mode.

A mm-wave gyro-TWA using a three-fold HCIR has been developed at The University of Strathclyde [18]. In previous gyro-TWA experiments, the measurement of the gain curve was carried out at discrete frequency points. This letter presents an upgrade of the gyro-TWA system, through the generation of an arbitrary waveform driving signal and an integrated data acquisition and processing system. This demonstrated the capability of the gyro-TWA to amplify nanosecond-scale frequency-swept signals (chirp signals), which is important for applications such as radar, telecommunication, and ESR. Amplification of sub-nanosecond pulses has been demonstrated by a gyro-TWA for the application of pulsed dynamic nuclear polarization and achieved an instantaneous frequency bandwidth (IFB) of 8 GHz with a central operating frequency of 250 GHz [19]. Therefore the shortest pulse it can amplify is ~125 ps (=1/IFB). The gyro-TWA experiment results reported in our previous experiments [18] can achieve an instantaneous bandwidth of ~9 GHz at a central frequency ~100 GHz which means it can amplify a pulses as short as ~110 ps, or 27 ps if it could be scaled to operate at 250 GHz.

II. Experiment setup for the W-band gyro-TWA

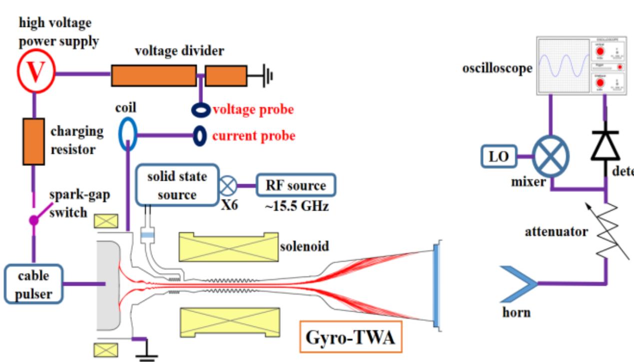

Fig. 1 The experimental setup of the Gyro-TWA. The detail of each component in gyro-TWA can be found in [18].

The experiment setup is shown in Fig. 1. The gyro-TWA contained key components including cusp electron gun [20], input coupler [21], elliptical polarizer, input and output windows [22], HCIR, and the solenoid system. All the

This work was supported by EPSRC UK (research Grant No. EP/G036659/1, EP/K029746/1) and STFC UK (research Grant No. ST/N002326/1 and ST/P001890/1). L. Zhang (liang.zhang@strath.ac.uk), C. R. Donaldson (craig.donaldson@strath.ac.uk), A. W. Cross (a.w.cross@strath.ac.uk), and W. He (w.he@strath.ac.uk) are with Department of Physics, SUPA, University of Strathclyde, Glasgow, G4 0NG, Scotland, UK. Peter Cain was with Keysight Technologies UK Ltd, Edinburgh EH12 9DJ, UK.

mm-wave components were optimized and verified by measurement using a vector network analyzer before and after they were assembled or vacuum brazed together. The input mm-wave signal was generated by a tunable solid-state amplifier (Quinstar QAR-90A12319Z10) with a maximum output power of 1.5 - 1.8 W at frequency range of 90 - 96.5 GHz. The output TE_{11} mode was converted into the Gaussian mode by a smooth-profiled horn [23] and coupled out by a three-disc mm-wave window [22]. A small proportion of the output mm-wave radiation was picked up by a standard W-band pyramid horn. In the initial experiments, the radiated power was measured by a calibrated crystal detector, and the frequency was measured by an in-band fundamental mixer and a digital storage oscilloscope.

The acceleration voltage between the cathode and anode was generated by a double-stacked Blumlein transmission line and a spark-gap switch. The axis-encircling electron beam was generated by an electron gun with a magnetic field reversal immediately in the front of the cathode. The beam velocity ratio, α (ratio of transverse velocity to axial velocity, v_t/v_z), could be tuned by changing the magnetic field at the cathode surface.

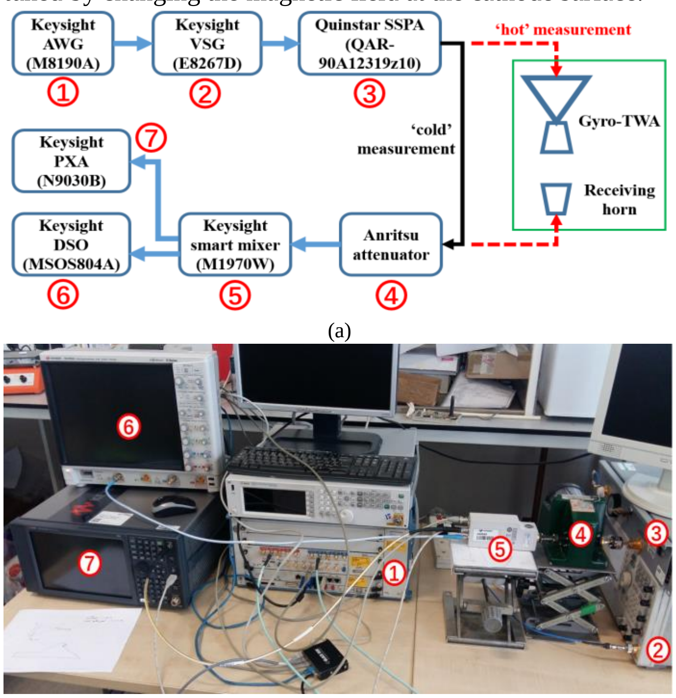

(a)

(b)

Fig. 2 A block diagram (a) and a photo (b) showing the setup for generation and measurement of the input mm-wave signal.

A block diagram describing the generation and measurement of the frequency-modulated input mm-wave signal is shown in Fig. 2(a). A Keysight arbitrary waveform generator (AWG, model M8190A) was used to generate arbitrary waveform up to 5 GHz analog bandwidth. It had a sample rate of up to 12 GSa/s and the amplitude of the signal could be controlled precisely and remotely. The signal was then modulated onto a ~15.5 GHz (when the central operating frequency was chosen to be 93 GHz) carrier signal generated by a vector signal generator (Keysight, model E8267D). The resultant mm-wave signal was then used as the input of the QuinStar solid-state amplifier which had a frequency multiplication of six times. In the "cold" measurement (when the gyro-TWA is turned off), the driving signal was measured by a waveguide harmonic mixer (Keysight M1970W) through an attenuator. Its frequency spectrum was measured by a signal analyzer (Keysight PXA N9030A) and the real-time signal was recorded by a digitizing oscilloscope (Keysight MSOS804A). A photo of the setup is shown in Fig. 2(b). The measurement setup provided a complete remote diagnostic solution that all these devices can be reconfigured or programmed. The acquired data was processed in real-time using 89600 VSA Software.

The input mm-wave signal was operated in continuous mode. The period of the frequency-swept signal was set around 200 ns which was shorter than the pulse length of the voltage pulse. Therefore, a full period of the input microwave signal can be captured within a single acceleration voltage pulse.

III. Simulation and Measurement Results

In the previous experiments [18], electron beam of 55 keV, 1.5A with an alpha of ~1.0 was used to achieve a gain of ~37 dB with a bandwidth larger than 5.5 GHz. To demonstrate the versatility in operating the gyro-TWA the beam voltage was lowered to 40 kV. The alpha value of the electron beam was also reduced to ~0.85 in order to match the dispersion of the operating eigenwave. The required magnetic field was accordingly adjusted to maintain the resonance between the electron beam mode and the eigenwave. The beam-wave interaction simulations with the new parameter sets were performed using 3D particle-in-cell code MAGIC. A lower gain of about 33 dB could be achieved in the similar frequency band if assuming an alpha spread of 10% and beam thickness of 0.1 mm.

Measurement results from the gyro-TWA experiment at a single frequency of 93 GHz are shown in Fig. 3. Before the acceleration voltage was applied, the spectrogram showed a major power burst at a frequency of 93 GHz in Fig. 3(a). The input mm-wave power received by the pyramid horn level is low, about -43 dBm, due to the long distance between the gyro-TWA and the horn. The amplified signal had strongest components at the same frequency after amplification by gyro-TWA, as can be seen in the spectrum plot in Fig. 3(c). A correlation plot of the mm-wave signal and the acceleration voltage is shown in Fig. 3(b). The first part of the voltage pulse was ~36 kV, nearly 10% lower than the second half. Although it did not affect the interaction frequency, it had a significant impact to the output power, which caused about -5 dB less power than at the beam voltage of 40 kV. The gain was calculated from the difference between the power levels with and without the operation of the gyro-TWA, and was found to be about 33 dB. There were mm-wave components at other frequencies at both ends of the pulse. They are caused by the oscillation at the rise and fall edges of the acceleration voltage. At lower voltage, the oscillation frequency was slightly higher because the relativistic factor was smaller and this results in an increase of the cyclotron frequency.

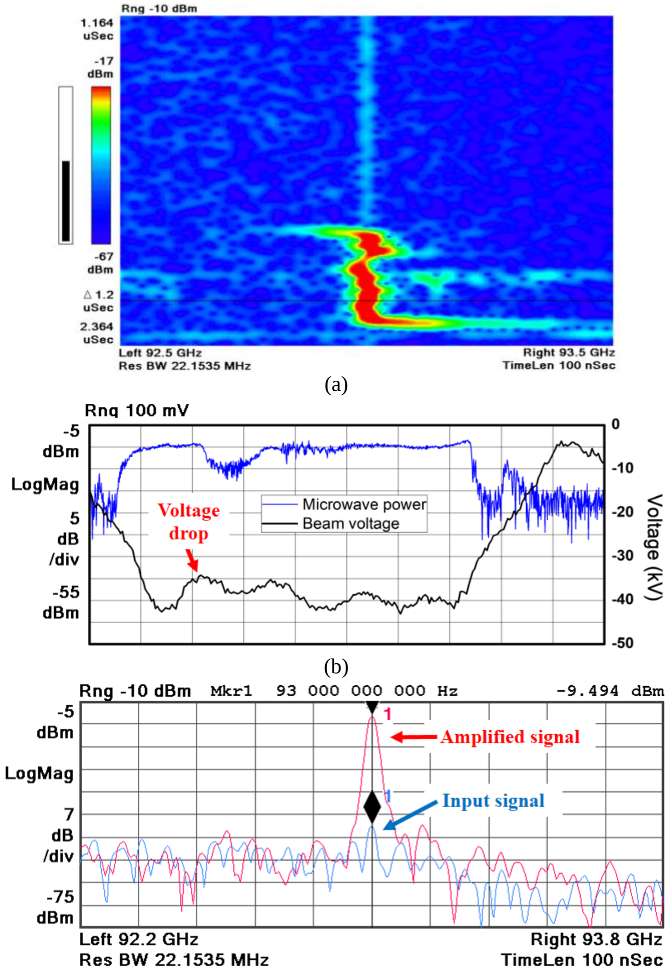

Fig. 3 Gyro-TWA experimental results at 93 GHz. (a) spectrogram, (b) correlation plot of the mm-wave signal and the acceleration voltage, and (c) spectrum of the mm-wave signal.

In a second experiment, a frequency-swept signal was set to a bandwidth of 1.0 GHz at the central frequency of 93.5 GHz. In Fig. 4(a), the frequency-swept signal generated from the solid-state source had larger noise than in the single frequency case due to the nonlinear behavior of frequency multipliers. The noise level was larger at the lower frequency than at the higher frequency. The amplified signal (Fig. 4(a)) showed clear frequency sweeping that aligned well with the input signal. The amplitude changes were due to the variations in the beam voltage. The spectrum of the amplified mm-wave signal in Fig. 4(b) showed a bandwidth close but smaller than 1 GHz. To identify the problem, the data of the input signal and the amplified signal was exported and the phase information was subtracted and is shown in Fig. 5. The solid-state source had larger phase distortion at a larger modulation frequency, while matched reasonably well at a small modulation frequency range. It is the major reason for the bandwidth narrowing. The phase information from the amplified signal of the gyro-TWA had the same trend as the input mm-wave signal. However, it had much bigger noise which was most caused by the variation of the beam voltage.

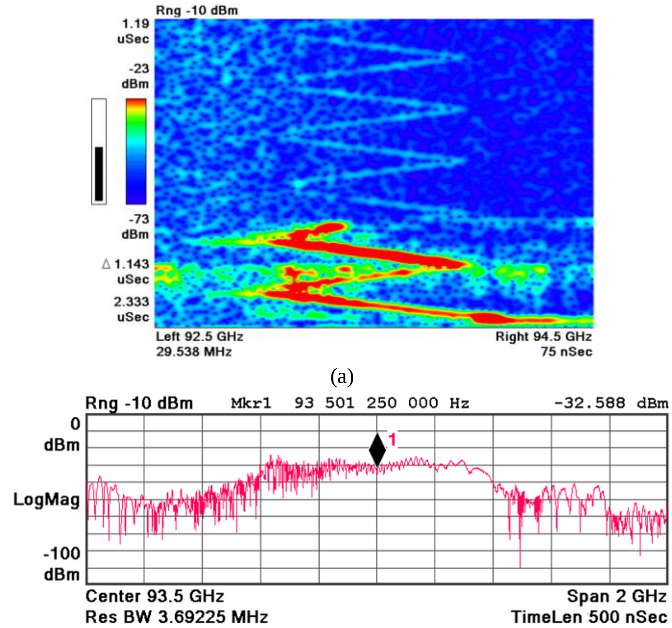

Fig. 4 Gyro-TWA experimental results with frequency-swept signal. (a) spectrogram, and (b) spectrum of the mm-wave signal.

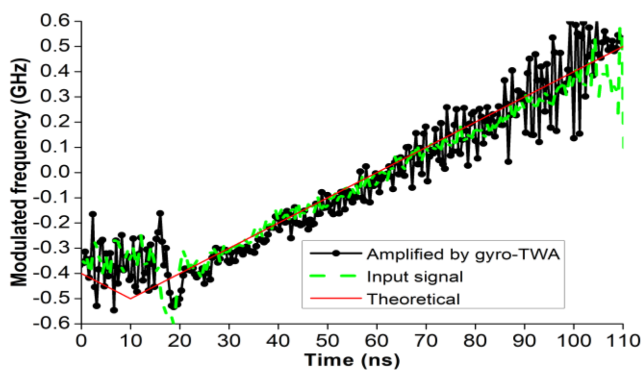

Fig. 5 Frequency sweeps of the input and output signal.

IV. Conclusion

In summary, proof-of-principle amplification of frequency swept signal in W-band has been carried out using a gyro-TWA. Frequency swept signal with a bandwidth of 1 GHz was generated as the input signal and the signal and successfully amplified with a gain of over 30 dB. The measured results were in excellent agreement with the simulation. The verification of the frequency agility of the W-band gyro-TWA enabled the possibility to carry out experiments for applications in the area of radar, communications and ESRS.

It was found that the nonlinear behavior from the solid state components, especially the frequency multipliers within the QuinStar amplifier, limited the measurements over an even wider bandwidth. Acquirement of a solid-state source with wider bandwidth and operation of the gyro-TWA with a much smaller variation in beam voltage and lesser electrical noise are being pursued.

References

[1] G. Burt, L. Zhang, D. A. Constable, H. Yin, C. J. Lingwood, W. He, C. Paoloni, and A. W. Cross, "A Millimeter-Wave Klystron

Upconverter With a Higher Order Mode Output Cavity," *IEEE Trans. Electron Devices,* vol. 64, no. 9, pp. 3857-3862, Sept. 2017. DOI: 10.1109/TED.2017.2724581

[2] K. R. Chu, "The electron cyclotron maser," *Rev. Mod. Phys.,* vol. 76, no. 2, pp. 489-540, May 2004. DOI: 10.1103/RevModPhys.76.489

[3] E. A. Nanni, S. M. Lewis, M. A. Shapiro, R. G. Griffin, and R. J. Temkin, "Photonic-Band-Gap Traveling-Wave Gyrotron Amplifier," *Phys. Rev. Lett.,* vol. 111, no. 23, p. 235101, Dec. 2013. DOI: 10.1103/PhysRevLett.111.235101

[4] H. H. Song, D. B. McDermott, Y. Hirata, L. R. Barnett, C. W. Domier, H. L. Hsu, T. H. Chang, W. C. Tsai, K. R. Chu, and N. C. L. Jr., "Theory and experiment of a 94 GHz gyrotron traveling-wave amplifier," *Physics of Plasmas,* vol. 11, no. 5, pp. 2935-2941, 2004. DOI: 10.1063/1.1690764

[5] V. L. Bratman, A. W. Cross, G. G. Denisov, W. He, A. D. R. Phelps, K. Ronald, S. V. Samsonov, C. G. Whyte, and A. R. Young, "High-Gain Wide-Band Gyrotron Traveling Wave Amplifier with a Helically Corrugated Waveguide," *Phys. Rev. Lett.,* vol. 84, no. 12, pp. 2746-2749, 2000. DOI: 10.1103/PhysRevLett.84.2746

[6] L. Zhang, W. He, K. Ronald, A. D. R. Phelps, C. G. Whyte, C. W. Robertson, A. R. Young, C. R. Donaldson, and A. W. Cross, "Multi-Mode Coupling Wave Theory for Helically Corrugated Waveguide," *IEEE Trans. Microwave Theory Techn.,* vol. 60, no. 1, pp. 1-7, Jan. 2012. DOI: 10.1109/TMTT.2011.2170848

[7] G. G. Denisov and M. G. Reznikov, "Corrugated cylindrical resonators for short-wavelength relativistic microwave oscillators," *Radiophysics and Quantum Electronics,* journal article vol. 25, no. 5, pp. 407-413, May 1982. DOI: 10.1007/bf01035315

[8] S. V. Mishakin and S. V. Samsonov, "Analysis of Dispersion and Losses in Helically Corrugated Metallic Waveguides by 2-D Vector Finite-Element Method," *IEEE Trans. Microwave Theory Techn.,* vol. 59, no. 9, pp. 2189-2196, Sept. 2011. DOI: 10.1109/TMTT.2011.2160201

[9] W. He, A. W. Cross, A. D. R. Phelps, K. Ronald, C. G. Whyte, S. V. Samsonov, V. L. Bratman, and G. G. Denisov, "Theory and simulations of a gyrotron backward wave oscillator using a helical interaction waveguide," *Appl. Phys. Lett.,* vol. 89, no. 9, p. 091504, 2006. DOI: 10.1063/1.2345607

[10] W. He, C. R. Donaldson, L. Zhang, K. Ronald, P. McElhinney, and A. W. Cross, "High Power Wideband Gyrotron Backward Wave Oscillator Operating towards the Terahertz Region," *Phys. Rev. Lett.,* vol. 110, no. 16, p. 165101, 2013. DOI: 10.1103/PhysRevLett.110.165101

[11] A. W. Cross, W. He, A. D. R. Phelps, K. Ronald, C. G. Whyte, A. R. Young, C. W. Robertson, E. G. Rafferty, and J. Thomson, "Helically corrugated waveguide gyrotron traveling wave amplifier using a thermionic cathode electron gun," *Appl. Phys. Lett.,* vol. 90, no. 25, p. 253501, 2007. DOI: 10.1063/1.2749425

[12] S. V. Samsonov, I. G. Gachev, G. G. Denisov, A. A. Bogdashov, S. V. Mishakin, A. S. Fiks, E. A. Soluyanova, E. M. Tai, Y. V. Dominyuk, B. A. Levitan, and V. N. Murzin, "Ka-Band Gyrotron Traveling-Wave Tubes With the Highest Continuous-Wave and Average Power," *IEEE Trans. Electron Devices,* vol. 61, no. 12, pp. 4264-4267, Dec. 2014. DOI: 10.1109/TED.2014.2364623

[13] G. G. Denisov, V. L. Bratman, A. W. Cross, W. He, A. D. R. Phelps, K. Ronald, S. V. Samsonov, and C. G. Whyte, "Gyrotron Traveling Wave Amplifier with a Helical Interaction Waveguide," *Phys. Rev. Lett.,* vol. 81, no. 25, pp. 5680-5683, Dec. 1998. DOI: 10.1103/PhysRevLett.81.5680

[14] S. V. Samsonov, A. D. R. Phelps, V. L. Bratman, G. Burt, G. G. Denisov, A. W. Cross, K. Ronald, W. He, and H. Yin, "Compression of Frequency-Modulated Pulses using Helically Corrugated Waveguides and Its Potential for Generating Multigigawatt rf Radiation," *Phys. Rev. Lett.,* vol. 92, no. 11, p. 118301, Mar. 2004. DOI: 10.1103/PhysRevLett.92.118301

[15] L. Zhang, S. V. Mishakin, W. He, S. V. Samsonov, M. McStravick, G. G. Denisov, A. W. Cross, V. L. Bratman, C. G. Whyte, C. W. Robertson, A. R. Young, K. Ronald, and A. D. R. Phelps, "Experimental Study of Microwave Pulse Compression Using a Five-Fold Helically Corrugated Waveguide," *IEEE Trans. Microwave Theory Techn.,* vol. 63, no. 3, pp. 1090-1096, 2015. DOI: 10.1109/TMTT.2015.2393882

[16] W. Lawson, M. R. Arjona, B. P. Hogan, and R. L. Ives, "The design of serpentine-mode converters for high-power microwave applications," *IEEE Trans. Microwave Theory Techn.,* vol. 48, no. 5, pp. 809-814, May 2000. DOI: 10.1109/22.841875

[17] G. G. Denisov, S. V. Samsonov, and D. I. Sobolev, "Two-dimensional realization of a method for synthesis of waveguide converters," *Radiophysics and Quantum Electronics,* journal article vol. 49, no. 12, pp. 961-967, Dec. 2006. DOI: 10.1007/s11141-006-0129-7

[18] W. He, C. R. Donaldson, L. Zhang, K. Ronald, A. D. R. Phelps, and A. W. Cross, "Broadband Amplification of Low-Terahertz Signals Using Axis-Encircling Electrons in a Helically Corrugated Interaction Region," *Phys. Rev. Lett.,* vol. 119, no. 18, p. 184801, Oct. 2017. DOI: 10.1103/PhysRevLett.119.184801

[19] E. A. Nanni, S. Jawla, S. M. Lewis, M. A. Shapiro, and R. J. Temkin, "Photonic-band-gap gyrotron amplifier with picosecond pulses," *Appl. Phys. Lett.,* vol. 111, no. 23, p. 233504, 2017. DOI: 10.1063/1.5006348

[20] C. R. Donaldson, W. He, A. W. Cross, F. Li, A. D. R. Phelps, L. Zhang, K. Ronald, C. W. Robertson, C. G. Whyte, and A. R. Young, "A cusp electron gun for millimeter wave gyrodevices," *Appl. Phys. Lett.,* vol. 96, no. 14, p. 141501, 2010. DOI: 10.1063/1.3374888

[21] L. Zhang, W. He, C. R. Donaldson, J. R. Garner, P. McElhinney, and A. W. Cross, "Design and Measurement of a Broadband Sidewall Coupler for a W-Band Gyro-TWA," *IEEE Trans. Microwave Theory Techn.,* vol. 63, no. 10, pp. 3183-3190, Oct. 2015. DOI: 10.1109/TMTT.2015.2464302

[22] C. R. Donaldson, P. McElhinney, L. Zhang, and W. He, "Wide-Band HE11 Mode Terahertz Wave Windows for Gyro-Amplifiers," *IEEE Transactions on Terahertz Science and Technology,* vol. 6, no. 1, pp. 108-112, June 2016. DOI: 10.1109/TTHZ.2015.2495221

[23] L. Zhang, W. He, C. R. Donaldson, G. M. Smith, D. A. Robertson, R. I. Hunter, and A. W. Cross, "Optimization and Measurement of a Smoothly Profiled Horn for a W-Band Gyro-TWA," *IEEE Trans. Electron Devices,* vol. 64, no. 6, pp. 2665-2669, June 2017. DOI: 10.1109/TED.2017.2687949